

Exploring organo-bentonite adsorption properties for biphenyl removal from organic-aqueous media: kinetic study and industrial perspective

Explorando as propriedades de adsorção da organo-bentonita para a remoção de bifênil de meios orgânicos-aquosos: estudo cinético e perspectiva industrial

DOI:10.34117/bjdv9n11-039

Recebimento dos originais: 13/09/2023

Aceitação para publicação: 14/10/2023

Chems Eddine Gherdaoui

PhD in Chemistry

Institution: Maxei Group

Address: 170 Allée de France, BP 22004, 62060 Arras - France

E-mail: chemseddine.gherdaoui@maxei.fr

Hussam Aldoori

PhD in Materials Chemistry

Institution: University of Lille - Unité Matériaux et Transformations (UMET)

Address: Univ. Lille, CNRS, INRAE, Centrale Lille, UMR 8207, F-59000

Lille - France

E-mail: hussam.aldoori@outlook.com

Chakib Alaoui

PhD in Materials Chemistry

Institution: Université des Sciences et de la Technologie d'Oran Mohamed Boudiaf -

Laboratoire de Chimie des Matériaux Inorganiques et Applications

Address: BP 1505, 31000 El-Mnaouer, Oran - Algeria

E-mail: chakib.alaoui@univ-usto.dz

Hanene Oumeddour

Master in Process and Environmental Engineering

Institution: University of Lille - Unité Matériaux et Transformations (UMET)

Address: Univ. Lille, CNRS, INRAE, Centrale Lille, UMR 8207, F-59000

Lille - France

E-mail: hanene.oumeddour@univ-lille.fr

Zohra Taibi

Master in Process Engineering

Institution: Université des Sciences et de la Technologie d'Oran Mohamed Boudiaf -

Laboratoire de Physico-Chimie des Matériaux-Catalyse et Environnement

Address: BP 1505, 31000 El-Mnaouer, Oran - Algeria

E-mail: taibi.zohramaster@gmail.com

Nouh Zeggai

PhD in Materials Chemistry
Institution: Université Paris-Saclay, ENS Paris-Saclay, CNRS
Address: 91190, Gif-sur-Yvette, France
E-mail: nouh.zeggai@ens-cachan.fr

Djahida Lerari

PhD in Materials Chemistry
Institution: Centre de Recherche Scientifique et Technique en Analyses Physico-chimiques (CRAPC)
Address: Zone Industrielle N 30, Tipaza, Bou-Ismaïl - Algérie
E-mail: djahida.lerari@crapc.dz

Ulrich Maschke

PhD in Materials Chemistry
Institution: University of Lille - Unité Matériaux et Transformations (UMET)
Address: Univ. Lille, CNRS, INRAE, Centrale Lille, UMR 8207, F-59000
Lille - France
E-mail: ulrich.maschke@univ-lille.fr

ABSTRACT

Biphenyl, a frequently encountered and resilient compound in wastewater, proves resistant to conventional treatment methods because of its enduring nature. It forms the structural basis for persistent organic pollutants such as PCBs. In this study, we explored the adsorption of biphenyl in an organo-aqueous medium using both natural (Bent) and organomodified (CTAB-Bent) bentonite clay. Our objective was to highlight its potential for biphenyl wastewater treatment. We analyzed the physicochemical and textural properties of these clays through FTIR, XRF, XRD, SEM, BET method, and Zeta potential measurements. Impressively, these materials exhibited remarkable biphenyl adsorption capacity under acidic conditions, with Bent achieving 60% removal and CTAB-Bent an impressive 91%. We investigated the adsorption kinetics using first-order and pseudo-second-order models and assessed isotherm data with the Langmuir, Freundlich, and Langmuir-Freundlich (sips) equations. The Langmuir model, at pH 3, proved optimal, with high accuracy (R^2) and minimal error (RMSE) values (0.997 and 1.20, respectively). Clay nature significantly influenced pollutant uptake efficiency, confirming the efficacy of the selected bio-based clay. We propose a protocol adaptable for industrial-scale applications.

Keywords: biphenyl, wastewater, adsorption treatment, organophilic clay, industrial conversion.

RESUMO

O bifênil, um composto frequentemente encontrado e resistente em águas residuais, demonstra ser resistente aos métodos de tratamento convencionais devido à sua natureza persistente. Ele forma a base estrutural para poluentes orgânicos persistentes, como os PCBs. Neste estudo, exploramos a adsorção do bifênil em meio orgânico-aquoso utilizando tanto argila bentonítica natural (Bent) quanto argila bentonítica organomodificada (CTAB-Bent). Nosso objetivo era destacar seu potencial para o tratamento de águas residuais contaminadas com bifênil. Analisamos as propriedades físico-químicas e texturais dessas argilas por meio de FTIR, XRF, XRD, SEM, método

BET e medições de potencial Zeta. De forma impressionante, esses materiais apresentaram uma notável capacidade de adsorção de bifenil em condições ácidas, com o Bent alcançando uma remoção de 60% e o CTAB-Bent um impressionante 91%. Investigamos a cinética de adsorção utilizando modelos de primeira ordem e pseudo-segunda ordem e avaliamos os dados de isoterma com as equações de Langmuir, Freundlich e Langmuir-Freundlich (sips). O modelo de Langmuir, a pH 3, provou ser o mais adequado, com valores de alta precisão (R^2) e erro mínimo (RMSE) (0,997 e 1,20, respectivamente). A natureza da argila influenciou significativamente a eficiência de remoção do poluente, confirmando a eficácia da argila de base biológica selecionada. Propomos um protocolo adaptável para aplicações em escala industrial.

Palavras-chave: bifenil, águas residuais, tratamento por adsorção, argila organofílica, conversão industrial.

1 INTRODUCTION

Non-halogenated aromatic cyclic molecules, such as biphenyls, have a longstanding history of utilization in the synthesis of organic products for the chemical industry. A notable example of this usage is in the production of polychlorinated biphenyls (PCBs). These compounds continue to be the subject of extensive research by various international entities, including state and municipal authorities [1] This scrutiny is driven by the well-documented toxic properties of PCBs, which present a direct threat to human health, whether through inhalation or indirectly via contamination of the food chain [2]. Despite the global ban on PCB production, large quantities of these Persistent Organic Pollutants (POPs) are still present in the environment [3]. It is important to note that PCBs are regarded as precursors for the formation of highly toxic substances, specifically polychlorinated dibenzofurans (PCDFs) and dibenzodioxins (PCDDs) [4,5]. These hazardous compounds can form spontaneously and uncontrollably when PCBs are released into the environment [6]. In this respect, the Stockholm Convention (2001) stipulated that PCBs should be phased out until 2028. However, their inventory shows that these molecules are still present due to intentional or unintentional releases in the environment [7,8]. The dechlorination of PCBs, whether anthropogenic or not, such as UV-Visible radiation, generates in most cases the biphenyl molecule, improperly called "PCB N°0" [9,10].

On the other hand, over the past 20 years, many scientific research papers have shown that clay-based materials are promising adsorbents for environmental applications such as water purifications of toxic organic compounds, especially surfactant-modified clays that have a higher adsorption capacity than the original clay [11,12]. However, most

of the work concerning the adsorption of organic compounds on clays has been carried out on functional molecules, comprising at least one OH function and/or one halogen atom [13–15] such as dyes [16,17]. In the case of biphenyl compounds, many articles mention the adsorption of chlorine-substituted biphenyl molecules in water, such as the work of S. Barreca and al. [18] which investigated the effect of montmorillonite in alginate gel beads for the adsorption of polychlorinated biphenyls in dilute solutions. In the research conducted by H. Song and al. they investigated the adsorption of polychlorinated biphenyls (PCBs) on gold colloids using surface-enhanced Raman spectroscopy (SERS) in combination with density functional theory (DFT) [19].

However, the adsorption has never been investigated on a molecule that has no functional group such as biphenyl. The latter may result from the treatment or degradation of organo-halogenated aromatic compounds (chlorinated or brominated) [20]. Furthermore, the majority of research focused on adsorption treatments of toxic molecules onto clays has been conducted within a singular solvent environment, predominantly either water or an organic solvent, with limited exploration of cosolvents [21,22].

Recently, water/THF mixture has been proved to act as a promising multifunctional solvent system for the fractionation of lignocellulose and solubilizing the resulted derivatives to obtain valuable chemicals with high yield and selectivity. Furthermore, the mixture water/THF proved to be an advantageous system for the recovery of biomass for the environment [23]. THF has been employed as a solvent and intermediate in industry for decades, owing to its low boiling point (66°C) and high vapor pressure (21.6 kPa at 25°C), which enable its easy recovery. In fact, THF is highly polar and miscible with water, forming an azeotrope with water [24,25]. Liu and al. [26] performed ab initio molecular dynamics simulations and proved that hydrogen bond was formed between the Hydrogen atom of water and Oxygen atom of THF with a 1.694 Å of bond length. However, Matouš and al [27] demonstrated that water/THF cosolvent had great positive deviations from Raoult's law to such degree.

In order to address the scientific question regarding the treatment of PCB N°0, a molecule with no functional group, such as biphenyl. In this article, we present a study focusing on the adsorption of biphenyl onto bentonite modified with cetyltrimethylammonium (CTAB) in a water/tetrahydrofuran (THF) mixture. We employed THF to solubilize biphenyl due to its low reactivity with water, primarily

attributed to the absence of functional groups [28]. Therefore, we added a fixed quantity of THF, representing the minimum solubility threshold of biphenyl, to the water.

The application of organophilic bentonite Bent-CTAB for removing biphenyl from the water/THF cosolvent involves two key steps. The first step comprises synthesizing organophilic bentonite through a process that involves pulverizing bentonite and mixing it with a surfactant solution for an extended duration [29]. The resulting product is characterized using various techniques, including X-ray diffraction, Fourier-transform infrared spectroscopy, and scanning electron microscopy. The second step entails using Bent-CTAB for the adsorption-based removal of biphenyl from the cosolvent.

This work also presents a study of biphenyl adsorption on the surfaces of both Bentonite Bent and Bent-CTAB in an acidified mixture consisting of 70% water and 30% THF at varying pH levels. The selection of an acidic pH is based on consistent findings from previous research, indicating that this pH range yields the highest adsorption efficiency [30,31]. Additionally, our study demonstrates that the adsorption efficiency of biphenyl on the Bent-CTAB organophilic clay is greater at pH = 3 compared to pH = 6 (the initial pH of the water/THF mixture). CTAB significantly enhances both the adsorption capacity and selectivity of bentonite clay in the water/THF mixture.

Moreover, to the best of our knowledge, the study of biphenyl adsorption on an organo-modified clay in a water/THF mixture has never been previously conducted on an industrial scale using a method that allows for the regeneration of the adsorbent. In this manuscript, based on the experimental results obtained, we propose a process that not only facilitates the industrial-scale application of this PCB No.0 treatment method but also enables the regeneration of the adsorbent.

2 EXPERIMENTAL PART

2.1 MATERIALS

The Bentonite clay employed in this research is sourced from Maghnia, a city situated in the western region of Algeria. The adsorbate selected in this study is biphenyl (PCB No. 0), supplied by Sigma-Aldrich. Which form the basic structure of polychlorinated biphenyls (PCBs). The surfactant cetyltrimethylammonium bromide (CTAB) ($C_{19}H_{42}NBr$, 99% provided by Sigma-Aldrich). Tetrahydrofuran (THF) was obtained from Sigma Aldrich in HPLC quality. All reagents were used as received without further purification.

2.2 PREPARATION OF ORGANOPHILIC CLAY ADSORBENTS

The starting clay used in this study is sourced from Maghnia. This clay has undergone a modification protocol composed of several stages: The first step is to saturate the dispersed clay with sodium using sodium chloride (0.1N). The obtained sodium bentonite was washed with water several times and dried at room temperature. The second step is to organo modify the sodic bentonite using cetyltrimethylammonium bromide (CTAB) ($C_{19}H_{42}NBr$, 99% provided by Sigma-Aldrich) as a cationic surfactant. Organic clay (Bent-CTAB) was prepared by the substitution of inorganic cations Na^+ of sodic bentonite by the quaternary ammonium cations, according to the procedure described by the recommended method of Bartelt-Hunt [32,33]. The amount of organic cations added is determined using equation (1), to achieve 300% of the cation exchange capacity (CEC) of the original clay, established at 109.50 meq/100 g [34].

$$F = \frac{M_{cation}}{CEC * m_{clay} * W_{cation} * x} \quad \text{Eq.(1)}$$

Where:

F is the satisfactory fraction of the cation exchange capacity by the organic cation (dimensionless),
 M_{cation} is the mass of organic cation required to achieve the desired fraction of the cation exchange capacity (CEC) of the clay (equivalent gram / gram of clay),
 m_{clay} represents the mass of clay used,
 W_{cation} is the molecular weight of the organic cation (g/mol), and x constitutes the number of moles of charge per equivalent (1 mole / equivalent) for the cations used, in this study (1 mole / equivalent). Theoretically, the cation exchange capacity represents the maximum amount of organic cation that can be exchanged on the surface of the clay.

2.3 ADSORPTION EXPERIMENTS

The adsorption experiments were carried out on the biphenyl (adsorbate) dissolved in an organo-aqueous medium consisting of deionized water and THF (70%-30%) (pH=6). The defined initial concentration of biphenyl in water/THF is 20 mg/L. Adsorption was achieved by adding 20 g of Bent or Bent-CTAB in 20 l of organo-aqueous solution (Water 70% - 30% THF) of biphenyl and stirring the mixture at 298 °K for ~ 200 min. The mixture was magnetically stirred at a rate of 400 rpm. In preliminary adsorption, a negligible effect of the stirring rate was observed. The adsorption kinetics of the biphenyl solution were followed by regular sampling with a 10 ml syringe for more than 200 hr. The control of the concentrates before and after adsorption was carried out using a calibration curve. To describe the adsorption equilibrium at the liquid/solid interface,

the amount of solute adsorbed at equilibrium is expressed per unit of mass of adsorbent q_e (mg/g), as a function of the remaining concentration in the solution at equilibrium C_e (mg/L).

The equilibrium concentration of biphenyl, q_e (mg/g), was calculated from the following mass balance (Equation (2)):

$$q_e = (C_0 - C_e) \frac{V}{m} \quad \text{Eq. (2)}$$

Where:

V represents the volume of the solution (L), C_0 and C_e are initial and equilibrium concentrations of biphenyl (mg/L), respectively, and m stands for the mass of adsorbent (g).

The removal efficiency R (%), corresponding to the percentage of adsorbed biphenyl at equilibrium, was expressed as follows: (3) [38,39]:

$$R \% = \left(\frac{C_i - C_e}{C_i} \right) * 100 \quad \text{Eq. (3)}$$

Where:

C_i and C_e represent the initial and equilibrium concentrations of biphenyl in the Water/THF solution, respectively. Adsorption experiments were repeated five times.

The regeneration of the adsorbent is of paramount importance in practical applications. In order to assess the recycling capacity of the Bent and Bent-CTAB adsorbents, as well as to quantify the efficiency of Biphenyl removal, we conducted several cycles of adsorption and desorption. The desorption experiments of the compounds were carried out using exclusively distilled water and THF mixture as the solvent. This approach aims to preserve the integrity of the adsorbent.

2.4 CHARACTERIZATION

X-ray diffraction (XRD) measurements were recorded according to a Bruker Diffractometer D5000 using $\text{Cu K}\alpha$ radiation ($\lambda = 1.54 \text{ \AA}$) and equipped with a graphite dos-monochromator. Samples were scanned from 2° to 70° (2θ) with a step of 0.08° and a counting time of 4 seconds per step. The chemical composition of clay was obtained

using a fluorescence spectrometer (Bruker S2-Ranger equipped with an EDS detector). The results were reported in mass wt. % of oxides for the major elements. The surface of the clays and their porosity were measured by physisorption of nitrogen at -196°C using a Micromeritics Tristar 2 porosimeter. Before analysis, the sample is degassed at 120°C for 6.5 hours. Reflectance infrared spectra (ATR-FTIR) were collected on a Perkin Elmer Frontier FTIR (Thermo Electron Corporation), equipped with a Smart Orbit accessory; the spectra were recorded with a scan number of 16 in the range $400\text{-}4000\text{ cm}^{-1}$. The Bent and Bent-CTAB materials were subsequently analyzed by zetametry in a pH range between 3 and 11 in water/THF solution (70 %-30 %). These solutions remained stirring for 24 hours after pH adjustment. The objective of this analysis is to define the point of zero charge (pzc) of the clays.

The adsorbate equilibrium concentrations study was carried out $\lambda=250\text{ nm}$ using a UV-Vis spectroscopy (double beam CARY VARIAN). The experiments were conducted in isotherms at $23 \pm 1^{\circ}\text{C}$. The monitoring of the intense UV absorption band (S0-S3) at 250 nm, which represents the transition of type $\pi\text{-}\pi^*$ [40], has allowed to determine removal kinetics.

3 RESULTS AND DISCUSSIONS

3.1 CLAYS CHARACTERIZATION

The chemical composition (% Weight) of Bent and Bent-CTAB, determined by the X-ray fluorescence technique, is given in Table 1. Bent was characterized by high contents of SiO_2 and Al_2O_3 , which represent the main oxides. The predominance of silica (62.84%) and aluminum oxide (16.43%) indicates that this clay is an aluminosilicate. The yellow-reddish color of the clay is due to magnesium and iron oxides which are present at 8.5% and 5.04%, respectively. The overall composition of the other oxides (Na_2O , CaO , SO_3 and TiO_2) reached a percentage of 7% wt, by organo-modification of Bent with alkylammonium surfactant, substituted by compensating cations in the clay. The representative formulas of the clay Bent and Bent-CTAB were defined by the equations to calculate the molar mass M (4) and the number of atoms N of the clay mesh (5), highlighting the bonds between the different constituents of the clay.

Table.1 Chemical composition of Bent and Bent-CTAB (wt.%)

Oxide	SiO ₂	Al ₂ O ₃	MgO	Fe ₂ O ₃	Na ₂ O	CaO	ClO	SO ₃	TiO ₂	ZrO ₂
Bent %	62.84	16.43	8.50	5.04	3.40	2.15	0.47	0.16	0.56	0.17
Chemical formula	Si _{7.06}	Al _{1.08}	Mg _{1.43}	Fe _{0.21}	Na _{0.39}	Ca _{0.25}	Cl _{0.09}	S _{0.01}	Ti _{0.04}	Zr _{0.009}
Bent-CTAB %	61.19	15.30	5.97	5.00	2.76	0	0	0	0.46	0
Chemical formula	Si _{6.86}	Al _{1.00}	Mg _{1.00}	Fe _{0.21}	Na _{0.29}	C _{2.19}	Ti _{0.038}			

Source: Authors

The mass of the elementary mesh is expressed according to following equation:

$$M = N * V * \rho * 10^{-24} \quad \text{Eq.(4)}$$

With:

N the Avogadro number, V the volume of the mesh in Å³ (cell parameters of bentonite clay are a=5.3 Å, b=9.05 Å, c=9.55 Å) and ρ the density of the clay in g/cm³ which is equal to 2.44 g/cm³ in the anhydrous state.

The number of atoms in the mesh:

$$N = \frac{(Q * M)}{(100 * M_{AO})} \quad \text{Eq.(5)}$$

Where:

M_{AO} is the molar mass of the oxide “AO” and Q is the percentage by weight expressed as oxide.

Table.2 summarizes the surfaces, total pore volume and average pore diameter values of the studied clays. It should be noted that the average pore of Bent is larger than that of Bent-CTAB. These results suggest that quaternary ammonium salts are present in the interlayer domain but also on the surface of Bent-CTAB, The specific area (according to the BET method) of the Bent was determined at 89 m²/g, which is consistent with the results of Liu and Naidu (2014). During the phenomenon of nitrogen adsorption, the molecules of gaseous N₂ not only occupy the geometric outer surface but also penetrate the capillaries. The decrease in the specific surface area of Bent-CTAB compared to Bent can be attributed to the blocking effect of porous aggregates and the increase in particle aggregation. The surface area of the clay decreases due to organophilization, This observation aligns with prior findings [38,39].

Table 2. Specific area, pore volume and average pore diameter of Bent and Bent-CTAB.

Adsorbent	Specific Surface (m ² /g)	Porous Volume (cm ³ /g)	Average pore diameter (nm)
Bent	89.73	0.10	14.82
Bent-CTAB	27.81	0.06	11.85

Source: Authors

FTIR analysis (Fig.1.A), indicates that the Bentonite spectrum reveals a band at 3660 cm⁻¹ assigned to the OH-group between the tetrahedral and octahedral sheets of the bentonite structure, and wide absorption bands at 3450 cm⁻¹ corresponding to the overlapping asymmetric and symmetric (H–O–H) of water molecule [40]. Another weak band at 1630 cm⁻¹ can be attributed to the water molecules of the inner layer [41].

In addition, absorption bands were observed corresponding to the Si–O vibration ion in the SiO₄ tetrahedron at 466 cm⁻¹ (in plane bending vibration); The Octahedron Al–O vibration at 787 cm⁻¹ corresponde to metal oxygene vibration [42], and the peak at 1021 cm⁻¹ were attributed to the asymmetrical stretch Si–O–Al [43]. Once bentonite has been treated with CTAB, , new absorption bands appeared at 2920 cm⁻¹ and 2850 cm⁻¹, assigned to elongation vibrations of alkyles groups –CH₃ and –CH₂, respectively. A new absorption band appeared around 1489 cm⁻¹, relying on elongation vibrations of N-H of the ammonium ions, which confirming the successful organomodification of the Bent [44].

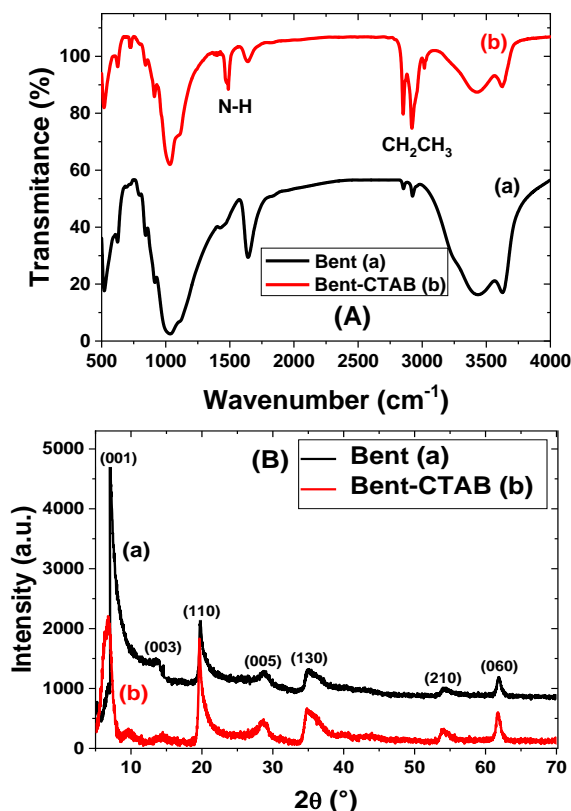
The X-ray diffraction diagram of the mineralogical phase of the clay samples (Fig.1.B) shows the presence of diffraction peaks at 2q = 5.91° (001), 19.69° (110) and 62.41 ° (060) which are characteristic of montmorillonite. The Bent- revealed the first basal reflection at $d_{001}=11.85 \text{ \AA}$, indicating that this clay is composed of completely collapsed layers with available interlayer space. Fig. 1.B shows a change in the number and height of peaks for Bent after modification with ammonium salts. The intensity of the peaks was found to be reduced for Bent-CTAB compared to Bent. This can be explained by the decrease in crystallinity created by the CTAB deposited at some sites on the surface of the Bent-CTAB clay. CTAB alkylammonium ions represent cationic surfactants that can easily attract a negative net charge of Bent The value of d_{001} changes for Bent-CTAB compared to Bent, indicating that the surfactant ions were interspersed in the interlayer space of the clay [40]. Indeed, layer spacing increased from 11.85 Å to 18 Å. This basal spacing corresponds to a bilayer of organic cations between the layers of the bentonite (thickness of about 7 Å). The increase in basal spacing of bentonite with CTAB (Bent-CTAB) cations can be attributed to the replacement of inorganic layer

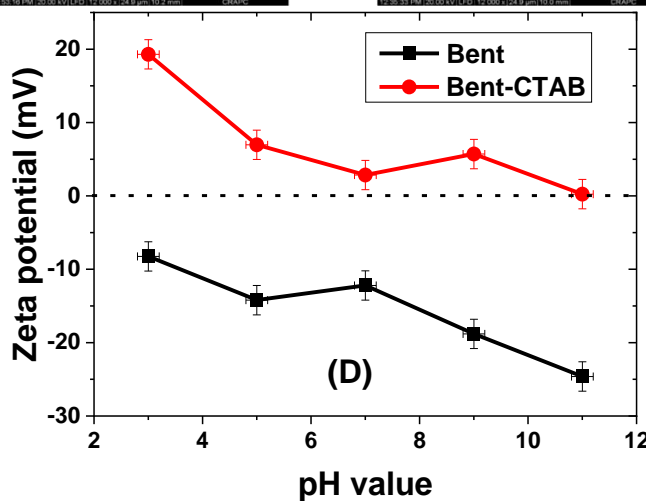
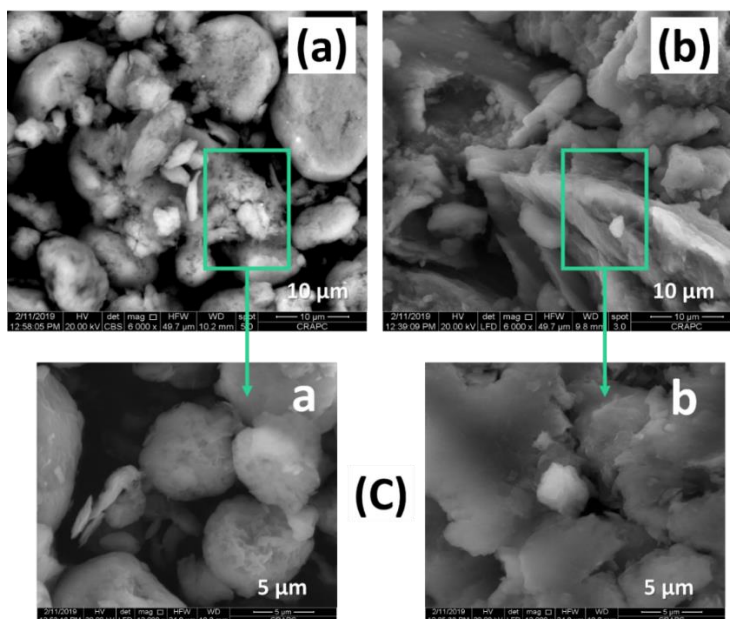
cations and their hydration water by CTAB cations [45]. Bentonite modification by CTAB was also associated with obvious changes in particle morphology and size. In this regard, SEM images of Bent and Bent-CTAB (Fig.1.C) show fewer agglomerates on the surface of the Bent material compared to the Bent-CTAB material. The latter contains in fact the particles of the CTAB on its surface which has been confirmed with the BET method

Fig.1.C (a) shows a laminar crystal structure characteristic of Bent phyllosilicates. After modification, it is observed in Fig.1.C (b) that the surfactant dominates the surface of the material Bent-CTAB and creates an agglomeration that is not seen on the material Bent illustrated in Fig.1.C (a) [46].

Figure 1.D illustrates the effect of zeta potential as a function of the clays pH. The material Bent does not show any pzc in a pH range between 3 and 11. This could be due to their permanent negative charges due to isomorphism substitution and/or structural defects. The material Bent-CTAB shows a positive zeta potential at different pH levels, probably because of the presence of the Quaternary ammonium cation (NR_4^+) of the Bent-CTAB. The pzc of this material is around $\text{pH} = 11$.

Figure 1 FTIR spectra (A), X-ray patterns (B), SEM images (C) and zeta potential (D) of Bent and Bent-CTAB; Ratio (water/THF) = 70/30.





Source: Authors

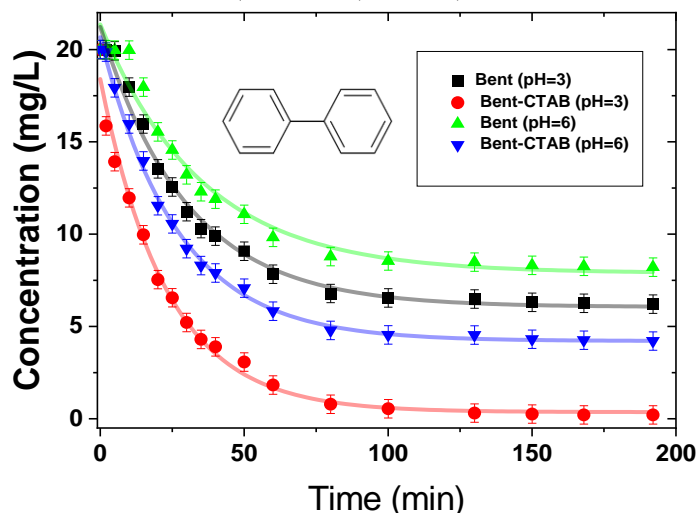
3.2 BIPHENYL ADSORPTION

The adsorption of biphenyl on Bent-CTAB can be explained in two ways, the first as the interaction of biphenyl in the interlamellar space (trapping of the molecule between the clay sheets) which is increased by the organo-modification, and the second is due to electrostatic interactions between the delocalized biphenyl electrons and the positive charges that cover the adsorbent [45,47].

Figure 2 shows the evolution of the biphenyl absorbance on water/THF solution (70:30) using the studied clays at pH=3 and pH=6. The pH value of the adsorption medium is generally the most important parameter affecting the adsorption capacity of materials. Indeed, the pH of the solution has a great influence on the surface of the clay, which subsequently leads to a change in the adsorption kinetics and equilibrium characteristics. From Fig.2 and in a pH range between 3 and 11, it can be concluded that

the pH value plays an important role in the rate and adsorption capacity of the biphenyl which is related to the surface of the material. The adsorption efficiency of this molecule increases by decreasing the pH solution. Indeed, at pH = 3, the biphenyl is more quickly adsorbed on the surface of Bent-CTAB positively charged, this phenomenon is explained by the forces of Van der Waals between delocalized electrons of aromatic rings and cations of bentonite. At pH values below 11, the surface of Bent-CTAB is positively charged, while that of Bent has a negative charge on the investigated pH values. Below a pH of 6, the neutral molecule of biphenyl tends to be adsorbed more efficiently on the modified bentonite via hydrophobic and Van der Waals interaction forces. Organo-modified bentonite exhibits surface hydrophobicity due to the presence of alkyl chains of surfactant. The long alkyl chain of CTAB (C₁₉) contributed to the increase in hydrophobic interactions, which could also explain the better adsorption of biphenyl on Bent-CTAB. The maximum adsorption in the pH range from 3.0 to 6.0 is due to the external electrostatic bonds formed on the surface of the Bent-CTAB, indeed the biphenyl molecule is stabilized via the interaction of π electrons of the cycle with the cations on the surface of the material [48].

Figure 2 Biphenyl concentration as function of adsorption time on Bent, and Bent-CTAB samples. Experimental conditions: C₀ = 20 mg/L; ms = 1 g/L; contact time t = 195 min; T = 298 ± 1 K; Ratio (water/THF) = 70/30



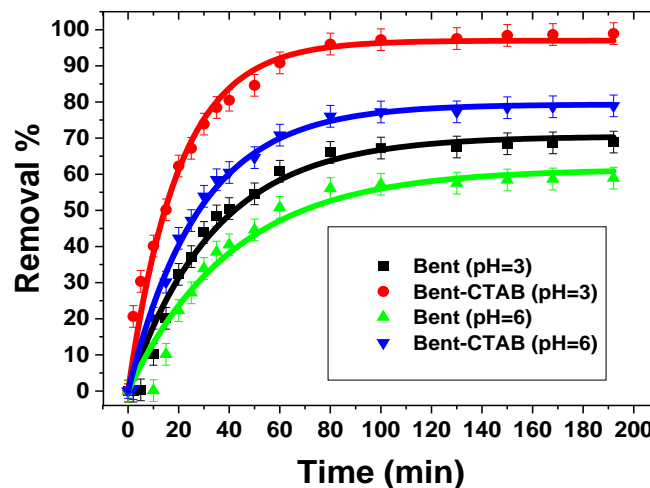
Source: Authors

The biphenyl molecule exists mainly in neutral form in the medium (water pK_a = 0 / THF pK_a = -2.08) despite the lower pK_a of these two solvents compared to the adsorbed molecule. Adsorption tests results have revealed that, at pH= 6 (the initial pH of the solution), the elimination percentage after 60 min of contact is 50% and 71% for

Bent and Bent-CTAB, respectively (Fig.3). At pH=3 and for the same time contact, the elimination percentage for the Bent material is 60% and 91% for Bent-CTAB, respectively.

The treatment efficiency is more important with Bent-CTAB at pH=3. This is due to the influence of intercalated and deposited quaternary ammonium on the interlayer clay spacing as well as the surface. These results correlate with those obtained in literature [45,49] which confirmed that the more acidic the medium, the higher the adsorption efficiency [50].

Figure 3. Effect of pH on the percentage of adsorbed biphenyl on Bent-, and Bent- samples (experimental conditions: $C_0 = 20 \text{ mg/L}$; $m_s = 1 \text{ g/L}$; contact time $t = 190 \text{ min}$; $T = 298 \pm 1 \text{ K}$; Ratio (water/THF) =70/30).



Source: Authors

3.3 ADSORPTION KINETICS

The adsorption kinetics of the biphenyl molecule was studied by applying two widely used models, the pseudo-first order model of Lagergren [51] and the model the pseudo-second order of Ho et al. [52]. It is described according to the following equations (6) and (7):

$$q_t = q_e(1 - e^{-k_1 t}) \quad \text{Eq. (6)}$$

$$q_e = \frac{k_2 q_2^2}{1 + k_2 q_2^2 t} \quad \text{Eq. (7)}$$

Where:

q_t is the adsorbed amount at any time t (mg/g), k_1 stands for the first-order rate constant (1/min), and k_2 is the second-order rate constant (g/mg·min).

It can be noted that adsorption kinetics were considered to compare the adsorption rates of Bent and Bent-CTAB. The influence of contact time on biphenyl removal (20 mg/L) at pH=6 and pH=3 at 20°C is illustrated in Fig.2 and Fig.3, and summarized in Table.3.

Table 3: Kinetic constants for pseudo-first- order and pseudo-second-order models for biphenyl adsorption on on Bent and Bent-CTAB.

Adsorbents	Pseudo first-order kinetic model		
	q_e (mg/L)	K_1 (min ⁻¹)	R_1^2
Bent (pH = 3)	14.10	0.029	0.979
Bent (pH = 6)	12.28	0.024	0.950
Bent-CTAB (pH = 3)	19.44	0.049	0.982
Bent-CTAB (pH = 6)	15.86	0.035	0.984
Adsorbent	Pseudo second-order kinetic model		
	q_e (mg/L)	K_2 (g/mg.min)	R_2^2
Bent (pH = 3)	16.86	0.0020	0.989
Bent (pH = 6)	15.17	0.0017	0.993
Bent-CTAB (pH = 3)	21.00	0.0030	0.994
Bent-CTAB (pH = 6)	18.43	0.0240	0.996

Source: Authors

It is evident that all samples successfully adsorb biphenyl with different efficiencies. The adsorption of biphenyl on Bent-CTAB is observed to be faster than that of Bent . In addition, the maximum amount of biphenyl adsorbed (q_e exp) (Fig .4) is higher for Bent-CTAB at pH=3 (21.50 mg/g) than for Bent-CTAB at pH=6 (16.43 mg/g), Bent at pH=3 (12.60 mg/g) and Bent at pH=6 (11.28 mg/g). These values of q_e (exp) closely matched the calculated q_e of the pseudo-second order model.

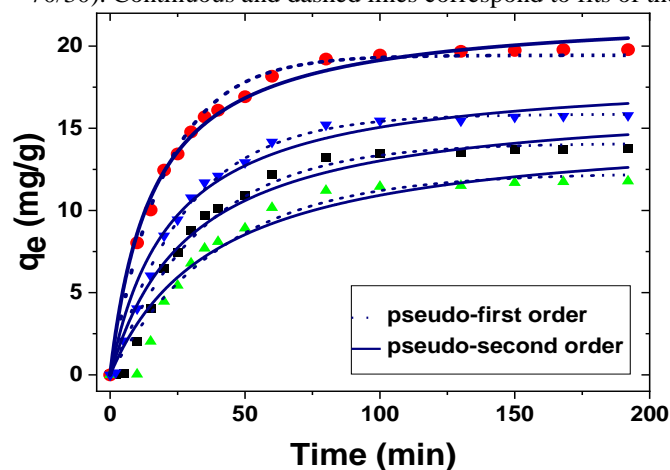
To achieve balance, it takes 70 to 80 min for Bent-CTAB and 60 min for Bent. The surface charge and the degree of ionization of the adsorbate are mainly responsible for the removal of biphenyl from the organoaqueous solution. The amount of adsorption increases with the increasing heterogeneity of the structure. The experimental data were adjusted using pseudo-first and pseudo-second order kinetic models, taking into account an initial biphenyl concentration of 20 mg/L.

The rate constants k_1 , k_2 and q_e , obtained from graphs applying equations (6) and (7) and q_e (exp) in Fig.4, as well as correlation coefficients R_1^2 and R_2^2 , are collected in Table 3. Accordingly, the kinetic data of Bent and Bet-CTAB followed the pseudo-second order model with high correlation coefficient (R_2^2) values of 0.989 and 0.993 respectively at pH=3 and pH=6 for Bent and 0.996 and 0.994 respectively at pH=3 and pH=6 for Bent-

CTAB, while the pseudo-first-order model gave R_1^2 values of 0.979, 0.950, 0.982 and 0.984, respectively.

Based on the consideration of biphenyl/adsorbent interactions, the pseudo-second-order model appears to be more appropriate than the pseudo-first-order model. The adsorption kinetics of biphenyl on clay generally follow the pseudo-second-order model [53]. From the literature, it is known the pseudo-first-order kinetic model can describe that physical adsorption, while the pseudo-second-order kinetic model can be applied to adjust chemical adsorption phenomena [53]. Indeed, biphenyl molecules are likely to hold several adsorption sites, instead of one, on solid surfaces[53]. As a result, Bent-CTAB at pH=3 has faster kinetics and higher adsorption capacity than other adsorbents. This means a stronger reaction between Biphenyl and some active sites of the same activity, unlike other sites on the surface of Bent.

Figure 4 Adsorption kinetics: effect of contact time of removal of biphenyl by Bent, and Bent-CTAB. Conditions: Biphenyl concentration 20 mg/L; adsorbent dosage ms = 1 g/L; pH =3 and 6; T=298 ± 1 K; Ratio (water/THF) = 70/30). Continuous and dashed lines correspond to fits of the experimental data.



Source: Authors

3.4 ADSORPTION ISOTHERM

The adsorption isotherm results were analyzed using Freundlich (Equation (8)), Langmuir (Equation (9)) and Sips (Langmuir-Freundlich)(Equation (10)) isotherms: [53,54], respectively:

$$q_e = K_f C_e^{1/n} \quad \text{Eq.(8)}$$

$$q_e = \frac{K_L q_m}{1 + K_L C_e} C_e \quad \text{Eq.(9)}$$

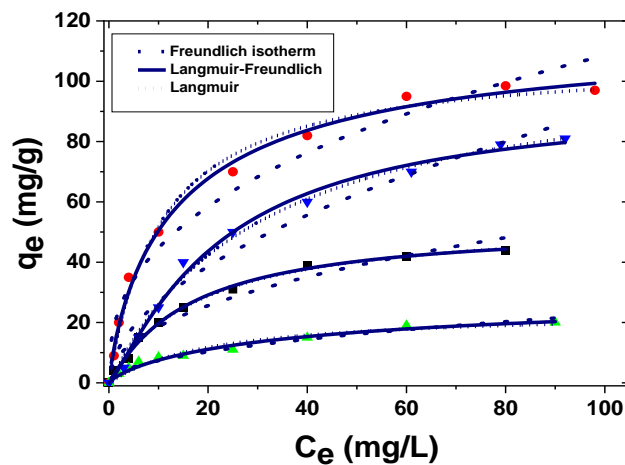
$$q_e = \frac{q_{smax} b_s C_e^\beta}{1 + b_s C_e^\beta} \quad \text{Eq.(10)}$$

Where:

k_f and $1/n$ are Freundlich constants related to adsorption capacity and adsorption intensity [55], respectively. q_m represents the monolayer adsorption capacity of the adsorbent, and k_L is the Langmuir constant related to the affinity of the binding sites (L/mg). q_{smax} corresponds to the Sips maximum.

The relationship between the amount of biphenyl adsorbed per adsorbent mass unit and its equilibrium concentration in solution is presented in Fig.5, in order to estimate the interaction between adsorbents and adsorbents. Moreover, Fig.5 shows a non-linear evolution of adsorption isotherms with concave curvatures on the abscissa. It can also be observed that the amount of adsorbed biphenyl increases at low adsorbate concentration, indicating that adsorption sites are available in excess, and saturation was achieved gradually with increasing adsorbate concentration. The lowest elimination of biphenyl was obtained using Bent as adsorbent at pH=6 and then pH=3. Larger amounts of biphenyl were adsorbed by Bent-CTAB, respectively at pH=6 and pH=3. In the range of concentrations between 10 and 180 mg/L, Bent and Bent-CTAB eliminate 12.74% and 51.40% respectively. The adsorption capacity of Bent is lower than that of Bent-CTAB regardless of the pH, due to their different hydrophobicities, since the surface of Bent-CTAB clay is not important. Thus, biphenyl was essentially adsorbed on organo-activated Bent-CTAB via hydrophobic and organophilic interactions.

Figure 5 Adsorption isotherms of biphenyl removal on Bent and Bent-CTAB samples. Conditions: $C_0=10$ to 180 mgL^{-1} ; adsorbent dosage $m_s= 1\text{g/L}$; pH=3, 6; $T= 298 \pm 1 \text{ K}$; Ratio (water/THF) = 70/30)



Source: Authors

The non-linear form of the Langmuir, Freundlich, and Langmuir-Freundlich (Sips) models was used to examine the experimental data on the adsorption of biphenyl, in order to obtain a better understanding of the possible adsorption mechanism. The parameters obtained from these isotherms were collected in Table 4.

Therefore, Langmuir isotherms correspond very well to experimental data for Bent and Bent-CTAB, with high and low R^2 and RMSE (Root Mean Square Error) values. In addition, a good agreement was found between the corresponding values of the calculated maximum adsorption capacity (q_{max}) of the Langmuir model and the experimental data, confirming that this model adequately describes the biphenyl adsorption process. The Langmuir model considers the surface homogeneous, so the adsorption of biphenyl on modified bentonite can be considered as single-layer adsorption without interaction between adsorbed molecules, since the adsorbent and the adsorbent interact strongly [56].

As a conclusion for this part, Bent-CTAB has a significantly higher adsorption capacity of biphenyl, unlike Bent regardless of pH.

Table 4: Freundlich, Sips and Langmuir parameters isotherms models for biphenyl adsorption on Bent and Bent-CTAB.

Isotherms	Parameters	Adsorbents			
		Bent		Bent-CTAB	
Freundlich (F)	pH	3	6	3	6
	$k_f(mg/g)^{1-1/n}$	6.54	2.37	18.41	8.00
	$1/n$	0.45	0.49	0.39	0.52
	R^2	0.955	0.950	0.955	0.96
	RMSE	11.35	2.52	64.46	34.57
Sips (L-F)	$q_s, max (mg/g)$	52.71	94.36	118.89	31.24
	b_s	0.053	0.023	0.110	0.049
	B	1.05	1.21	0.84	0.80
	R^2	0.994	0.930	0.991	0.959
	RMSE	1.46	6.41	12.26	1.99
Langmuir (L)	$q_L, max (mg/g)$	54.27	24.03	108.00	107.94
	$k_L(L/mg)$	0.057	0.048	0.093	0.032
	R^2	0.996	0.967	0.997	0.993
	RMSE	1.20	1.62	13.63	7.47

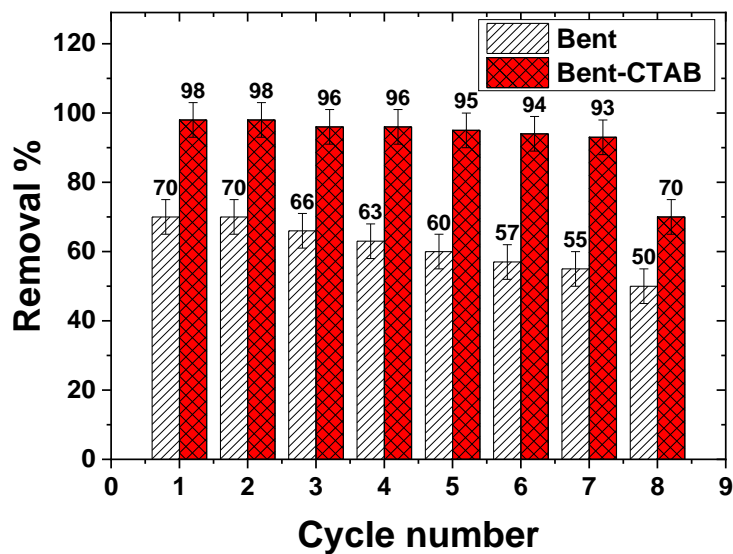
Source: Authors

3.5 ADSORBENTS REGENERATION CYCLES AND INDUSTRIAL TRANSPOSITION

To assess its suitability for industrial integration, we undertook a thorough examination covering 8 adsorption cycles [57]. This effort aimed to assess the potential for reuse of the adsorbent.

The adsorption capacity of Bent and Bent-CTAB was reduced after eight cycles. Indeed, the adsorption efficiency decreased from 70% to 50% for Bent while that of Bent-CTAB the efficiency decreased from 98% to 70%. Bent-CTAB remains stable for 7 cycles and its efficiency remains quite high despite the 28% decrease. Bent gradually decreases from one cycle to the next and this is the big difference between the two clays (Fig.6).

Figure 6 Cycles regeneration of Bent and Bent-CTAB for biphenyl adsorption



Source: Authors

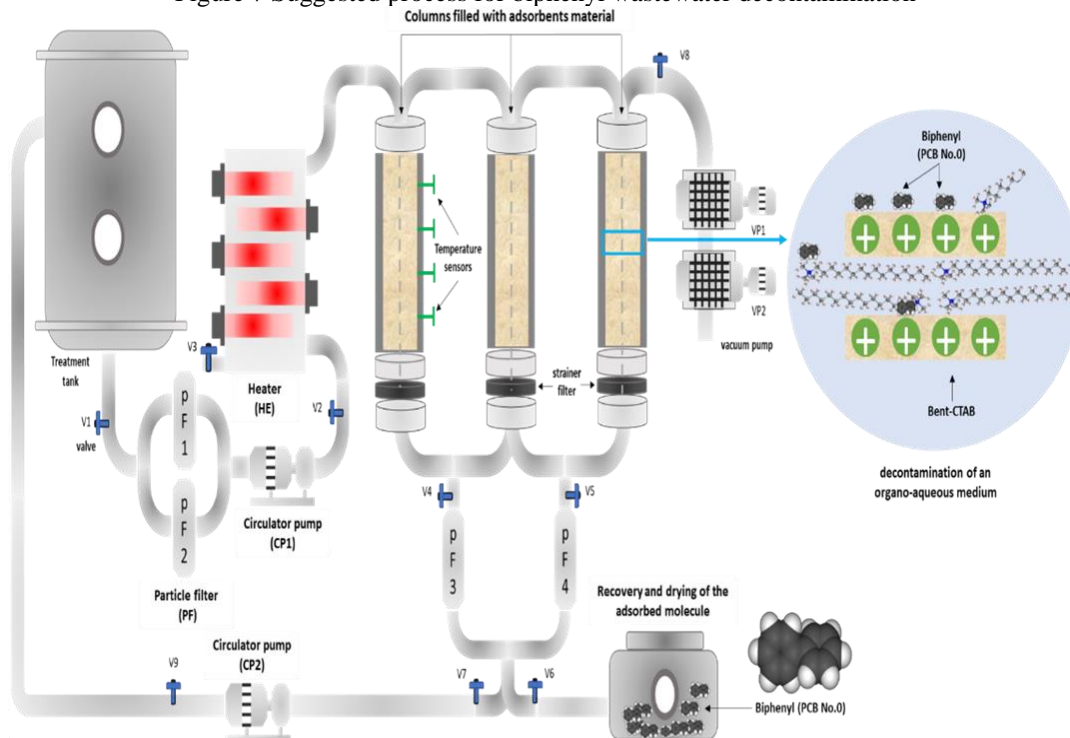
Based on the obtained result, it is suggested to translate the decontamination of biphenyl wastewater to an industrial scale. The process for the treatment of aqueous organic liquids (Fig.7) consists of two phases, the liquid decontamination phase and the adsorbent regeneration phase. During the water decontamination phase, the biphenyl-contaminated aqueous-organic liquid is pre-filtered at the inlet of the apparatus by a cartridge filter (PF1/PF2), and then it is sucked by the introduction pump (CP1) and heated by immersion heaters through the electric boiler (HE). After filtration, the liquid is injected into the columns filled with Bent-CTAB.

At its exit, the fluid passes through a second filtration (1 μ nominal cartridge) before being returned to the treatment tank by the extraction pump (CP2) through the valve (V7). This process is repeated in a closed loop until the desired biphenyl concentration is reached. As the aqueous-organic liquid passes through the columns, the Bent-CTAB adsorbs the biphenyl molecules contained in the liquid and gradually

becomes saturated. When the degree of saturation is achieved, the regeneration process must be started in order to restore the adsorbing properties of Bent-CTAB.

The regeneration process of Bent-CTAB consists in passing air through the valve (V3) and the vacuum pump (VP1/VP2), the air heated to 255 °C by the immersion heaters through the electric boiler (CE) enters the Bent-CTAB columns under vacuum and desorbs the biphenyl molecules. Once released from the active site of the adsorbent under the effect of the ambient air, the biphenyls will be carried towards the drying tank through the valve (V6).

Figure 7 Suggested process for biphenyl wastewater decontamination



Source: Authors

4 CONCLUSION

The present study revealed that the modification of Bentonite (Bent) by quaternary ammonium (CTAB) makes it possible to obtain considerable amounts of organic carbon, estimated at 14 %.

The SEM images and the absorption bands corresponding to the C–C fraction and the C–H vibrations observed by FTIR confirm the quaternary ammonium presence on the surface of the modified clay, while XRD analysis shows that quaternary ammonium is also integrated in the inter-foil space of the modified clay. Organo-bentonite Bent-CTAB showed improved adsorption capabilities compared to unmodified bentonite Bent.

Biphenyl (PCB No.0) has been found to have an improved adsorption behavior on Bent-CTAB compared to Bent. The adsorption capacity of the biphenyl increases in the presence of CTAB at pH = 3. These results are due to the increased electrostatic attraction between the π electrons of the biphenyl molecule and the positive charges on the surface of the Bent-CTAB. The kinetics of PCB No.0 on Bent and, Bent-CTAB follow a pseudo-second-order model. It is also stated that the effectiveness of the treatment is better at a strongly acidic pH (pH = 3). The results obtained could be well described by Langmuir's isotherm model. The study of industrial transposition is being improved near the R&D department of the company Arras Maxei. Preliminary results are satisfactory.

ACKNOWLEDGMENTS

The authors would like to express their gratitude to Dr. Christel Pierlot and Pr. Philippe Supiot from the University of Lille for their invaluable support.

This project received funding from the Arras Maxei Group, for which we are profoundly thankful.

We would also like to thank Jean-Philippe Delbarre, Stéphane Merlot, Roger Sansano and Olivier Hutin for their very productive collaboration at the laboratory and industry level, which contributed significantly to the success of this work.

REFERENCES

1. Gorbunova, T. I.; Kozhevnikova, N. S.; Vorokh, A. S.; Enyashin, A. N.; Pervova, M. G.; Zapevalov, A. Ya.; Saloutin, V. I.; Chupakhin, O. N. ;*Reac Kinet Mech Cat* 2019, 126, 1115.
2. Fürst, P. In *Encyclopedia of Food Chemistry*; Elsevier, 2019; pp. 384–392.
3. Gherdaoui, C. E.; Bouberka, Z.; Delbarre, J.-P.; Hutin, O.; Sansano, R.; Leclercq, L.; Supiot, P.; Maschke, U. ;*Waste Manag Res* 2022, 0734242X2211054.
4. Wu, B.-Z.; Chen, H.-Y.; Wang, S. J.; Wai, C. M.; Liao, W.; Chiu, K. ;*Chemosphere* 2012, 88, 757.
5. Pongpiachan, S.; Wiriwutikorn, T.; Phetsomphou, P.; Jieam, K.; Vongxay, K.; Choviran, K.; Sbrilli, A.; Gobbi, M.; Centeno, C. ;*Data in Brief* 2019, 22, 286.
6. Fiedler, H. In *The Fate of Persistent Organic Pollutants in the Environment*; Mehmetli, E.; Koumanova, B., Eds.; NATO Science for Peace and Security Series C: Environmental Security; Springer Netherlands: Dordrecht, 2008; pp. 3–12.
7. Official Journal of the European Union Directive 2012/19/Eu of the European Parliament and of the Council of 4 July 2012 on Waste Electrical and Electronic Equipment (WEEE) (recast).
8. *Fundamental Texts On European Private Law*; Radley-Gardner, O.; Beale, H.; Zimmermann, R., Eds.; Hart Publishing, 2016.
9. Gherdaoui, C. E.; Bouberka, Z.; Supiot, P.; Maschke, U.; Delbarre, J.-P.; Hutin, O.; Sansano, R. Method for dechlorination of one or more aromatic organochlorine compound(s) contained in an oil or forming said oil - associated electrical/electronic device and installation 2021.
10. Hassan, S. S. M.; El-Shazly, A. N.; Ismael, A. M.; Yehia, M. M.; Kamel, A. H.; Rashad, M. M. ;*Optical Materials* 2023, 142, 114084.
11. Desai, H.; A, K.; Reddy, G. S. K. ;*Microporous and Mesoporous Materials* 2023, 352, 112488.
12. Monteiro, M. K. S.; de Oliveira, V. R. L.; dos Santos, F. K. G.; de Barros Neto, E. L.; de Lima Leite, R. H.; Aroucha, E. M. M.; de Oliveira Silva, K. N. ;*Journal of Molecular Liquids* 2018, 272, 990.
13. Liu, Z.; Zhang, G.; Wang, M. K. ;*Applied Clay Science* 2014, 101, 297.
14. Sharma, B.; Gardner, K. H.; Melton, J.; Hawkins, A.; Tracey, G. ;*Environmental Engineering Science* 2009, 26, 1279.
15. Yu, M.; Hunter, J. T.; Falconer, J. L.; Noble, R. D. ;*Microporous and Mesoporous Materials* 2006, 96, 376.

16. Naz, A.; Chowdhury, A. ;Materials Today: Proceedings 2022, 60, 1.
17. Labied, R.; Ouraghi, M.; Hazam, S.; Touahra, F.; Lerari, D. ;Journal of Molecular Structure 2022, 1269, 133863.
18. Barreca, S.; Orecchio, S.; Pace, A. ;Applied Clay Science 2014, 99, 220.
19. Song, H.; Yan, X.; Zhao, H.; Zhang, X.; Shi, X.; Ma, J. ;Vibrational Spectroscopy 2022, 120, 103369.
20. Zhao, Q.; Zhao, X.; Cao, J. In Advanced Nanomaterials for Pollutant Sensing and Environmental Catalysis; Elsevier, 2020; pp. 249–305.
21. Pálková, H.; Madejová, J.; Komadel, P. ;Open Chemistry 2009, 7, 494.
22. Awad, A. M.; Shaikh, S. M. R.; Jalab, R.; Gulied, M. H.; Nasser, M. S.; Benamor, A.; Adham, S. ;Separation and Purification Technology 2019, 228, 115719.
23. Li, J.; Zhang, W.; Xu, S.; Hu, C. ;Front. Chem. 2020, 8, 70.
24. Howard, P. H. 1990.
25. Isac-García, J.; Dobado, J. A.; Calvo-Flores, F. G.; Martínez-García, H. In Experimental Organic Chemistry; Elsevier, 2016; pp. 71–144.
26. Liu, J.; Yan, Y.; Yan, Y.; Zhang, J. ;Crystals 2019, 9, 73.
27. Matous, J.; Novak, J. P.; Sobr, J.; Pick, J. .
28. Kumar Trivedi, M. ;AJCHE 2015, 3, 58.
29. Smith, J. A.; Jaffe, P. R. ;Environ. Sci. Technol. 1991, 25, 2054.
30. Smith, J. A.; Galan, Adina. ;Environ. Sci. Technol. 1995, 29, 685.
31. Khenifi, A.; Bouberka, Z.; Bentaleb, K.; Hamani, H.; Derriche, Z. ;Chemical Engineering Journal 2009, 146, 345.
32. Bartelt-Hunt, S. L.; Burns, S. E.; Smith, J. A. ;Journal of Colloid and Interface Science 2003, 266, 251.
33. Redding, A. Z.; Burns, S. E.; Upson, R. T.; Anderson, E. F. ;Journal of Colloid and Interface Science 2002, 250, 261.
34. Majdan, M.; Pikus, S.; Gajowiak, A.; Sternik, D.; Zięba, E. ;Journal of Hazardous Materials 2010, 184, 662.
35. Chinoune, K.; Bentaleb, K.; Bouberka, Z.; Nadim, A.; Maschke, U. ;Applied Clay Science 2016, 123, 64.

36. Touaa, N. D.; Bouberka, Z.; Gherdaoui, C. E.; Supiot, P.; Roussel, P.; Pierlot, C.; Maschke, U. ;Funct. Mater. Lett. 2020, 13, 2051008.
37. Shull, H. The Theory of the Electronic Spectra of Organic Molecules; Elsevier, 1964.
38. de Paiva, L. B.; Morales, A. R.; Valenzuela Díaz, F. R. ;Applied Clay Science 2008, 42, 8.
39. Lira Junior, C. A.; Silva, D. S. A.; Costa Filho, A. P. da; Lucas, E. F.; Santana, S. A. A. ;Journal of the Brazilian Chemical Society 2016.
40. Djomgoue, P.; Njopwouo, D. ;JSEMAT 2013, 03, 275.
41. Rashid, E. S. A.; Rasyid, M. F. A.; Akil, H. M.; Ariffin, K.; Kooi, C. C. ;Applied Clay Science 2011, 52, 295.
42. Alaoui, C.; Karmaoui, M.; Elaziouti, A.; Touati, W.; kaddi Allah, I.; Benhamed, A.; Bekka, A. ;Res Chem Intermed 2023, 49, 1213.
43. Bouberka, Z.; Khenifi, A.; Sekrane, F.; Bettahar, N.; Derriche, Z. ;Chemical Engineering Journal 2008, 136, 295.
44. Majdan, M.; Maryuk, O.; Gładysz-Płaska, A.; Pikus, S.; Kwiatkowski, R. ;Journal of Molecular Structure 2008, 874, 101.
45. Belaroussi, A.; Labed, F.; Khenifi, A.; Akbour, R. A.; Bouberka, Z.; Kameche, M.; Derriche, Z. ;Acta Ecologica Sinica 2018, 38, 148.
46. Akl MA Youssef AM; Al-Awadhi MM ;J Anal Bioanal Tech 2013, 04.
47. Pacios, L. F.; Gómez, L. ;Chemical Physics Letters 2006, 432, 414.
48. Wang, X.; Ling, S.; Guan, K.; Luo, X.; Chen, L.; Han, J.; Zhang, W.; Mai, B.; Zhou, B. ;Environ. Sci. Technol. 2019, 53, 8437.
49. Chiou, M.-S.; Chuang, G.-S. ;Chemosphere 2006, 62, 731.
50. Kameni, H.; Fouodjouo, M.; Zé, W.; Aldoori, H.; Gherdaoui, C. E.; Supiot, P.; Maschke, U.; Laminsi, S. ;Braz. J. Develop. 2023, 9, 7607.
51. Lagergren, S. ;Zeitschr f Chem und Ind der Kolloide 1907, 2, 15.
52. Ho, Y. S.; McKay, G. ;Process Biochemistry 1999, 34, 451.
53. Periasamy, K.; Namasivayam, C. ;Waste Management 1995, 15, 63.
54. Hameed, B. H.; Ahmad, A. A. ;Journal of Hazardous Materials 2009, 164, 870.
55. Silva, D. C. T. e; Silva, M. L. M. da; Medeiros, E. B. de M.; Filho, N. M. de L. ;Brazilian Journal of Development 2022, 8, 28877.

56. Bentaleb, K.; Boubarka, Z.; Chinoune, K.; Nadim, A.; Maschke, U. ;Journal of the Taiwan Institute of Chemical Engineers 2017, 80, 578.

57. Zeggai, N.; Boubarka, Z.; Dubois, F.; Bedjaoui, L.; Bouchaour, T.; Gherdaoui, C. E.; Potier, J.; Supiot, P.; Maschke, U. ;Composites Science and Technology 2022, 219, 109213.